© Koniaeva A.D., Varakuta E.Y., Leiman A.E., Bolbasov E.N., Stankevich K.S., 2022
DOI: 10.31088/CEM2022.11.1.50-61

# Changes in the cellular composition of the inflammatory infiltrate and connective tissue of the oral mucosa in rats during wound healing using a protective piezoelectric coating

***A.D. Koniaeva[1], E.Y. Varakuta[1], A.E. Leiman[1], E.N. Bolbasov[2], K.S. Stankevich[3]***

[1] Siberian State Medical University, Tomsk, Russia
[2] National Research Tomsk Polytechnic University, Tomsk, Russia
[3] Montana State University, Bozeman, MT, USA

**Abstract.** *Introduction.* Wound healing is a process based on a complex mechanism of intercellular interaction. The aim was to study changes in the oral mucosa cellular composition during wound healing with and without a protective piezoelectric coating.
*Materials and methods.* The study was carried out on 50 Wistar rats divided into four groups: one control group of intact rats and experimental groups 1, 2, and 3. The rats of the experimental groups were subjected to excision of a lip mucous membrane flap with wound formation. In the animals of experimental group 1, the defect was open. In group 2, we used a polymer membrane with copper modification, and in group 3, the membrane was without copper modification. The animals were sacrificed on days 3, 7, and 12 of the study. We used light and electron microscopy to study the qualitative and quantitative changes in the composition of cell populations at the site of the defect.
*Results.* On day 3, there prevailed neutrophilic infiltration in all groups. In groups 2 and 3, we observed a large number of macrophages and fibroblasts that indicated the transition to the next phase of wound healing. On day 7, in group 1, there persisted extensive neutrophilic and macrophage infiltration, whereas, in groups 2 and 3, the signs of inflammation decreased, and wound healing was active. On day 12, in group 1, all values were significantly higher than in the control group and there was damage to the ultrastructure; in groups 2 and 3, all the studied parameters reached the control values.
*Conclusion.* We revealed the patterns of changes in the cellular composition of a wound during its healing. The use of the coating contributed to accelerated wound healing, which was found during the analysis of changes in the composition of cell populations. The closure of the oral mucosa wounds with polymer piezoelectric membranes was proven to have a good effect on tissue repair and was supposed to reduce the risk of postoperative complications.

**Keywords:** wound defect, mucous membrane, oral cavity, piezoelectrics, inflammation, regeneration, scaffolds, dentistry

**Corresponding author:** Anastasiia D. Koniaeva. E-mail: asyakonya95@gmail.com

**For citation:** Koniaeva A.D., Varakuta E.Y., Leiman A.E., Bolbasov E.N., Stankevich K.S. Changes in the cellular composition of the inflammatory infiltrate and connective tissue of the oral mucosa in rats during wound healing using a protective piezoelectric coating. Clin. exp. morphology. 2022;11(1):50–61. DOI: 10.31088/CEM2022.11.1.50-61.

**Funding.** The study was carried out within the framework of state budget funding.

**Conflict of interest.** The authors declare no conflict of interest.

**Received** 27.12.2021. **Received in revised form** 25.01.2022. **Accepted** 28.02.2022.

УДК: 611.311

## Изменения клеточного состава воспалительного инфильтрата и соединительной ткани слизистой оболочки полости рта крыс при регенерации раны с использованием защитного пьезоэлектрического покрытия

***А.Д. Коняева[1], Е.Ю. Варакута[1], А.Е. Лейман[1], Е.Н. Больбасов[2], К.С. Станкевич[3]***

[1] ФГБОУ ВО Сибирский государственный медицинский университет Минздрава России, Томск, Россия
[2] ФГАОУ ВО Национальный исследовательский Томский политехнический университет, Томск, Россия
[3] Государственный университет штата Монтана, Бозмен, Монтана, США

*Введение.* Заживление раневого дефекта – комплексный процесс, в основе которого лежит сложный механизм межклеточного взаимодействия. Целью исследования являлось изучение изменения клеточ-

ного состава слизистой оболочки полости рта в ходе регенерации раневого дефекта при использовании защитного пьезоэлектрического покрытия и без него.

*Материалы и методы.* Исследование было проведено на 50 крысах линии Вистар, разделенных на четыре группы: контрольная – интактные животные, 1-я экспериментальная – животные с открытым раневым дефектом, 2-я и 3-я экспериментальные – животные с раневым дефектом, перекрытым полимерной мембраной без модификации и с медным напылением, соответственно. Забор материала для световой и электронной микроскопии проводили на 3-и, 7-е и 12-е сутки исследования. Изучали качественные и количественные изменения состава клеточных популяций на месте дефекта.

*Результаты.* На 3-и сутки исследования во всех группах преобладала нейтрофильная инфильтрация. Во 2-й и 3-й экспериментальных группах наблюдалось большое количество макрофагов и фибробластов, свидетельствующих о переходе на следующую стадию регенерации раны. На 7-е сутки в 1-й группе сохранялись обширная нейтрофильная и макрофагальная инфильтрация, во 2-й и 3-й группах признаки воспаления снижались, активно происходила регенерация раны. На 12-е сутки во 2-й и 3-й экспериментальных группах все исследуемые показатели достигали контрольных значений, в 1-й группе все значения были достоверно выше контрольных, имелись нарушения ультраструктурного строения клеток.

*Заключение.* В ходе исследования выявлены закономерности изменения клеточного состава раневого дефекта при его регенерации. Использование покрытия способствовало ускоренному заживлению раны, что было выяснено в ходе анализа изменения состава клеточных популяций. Доказано, что закрытие ран слизистой оболочки полости рта полимерными пьезоэлектрическими мембранами благоприятно влияло на восстановление целостности тканей и, предположительно, снижало риск возникновения послеоперационных осложнений.

**Ключевые слова:** раневой дефект, слизистая оболочка, полость рта, пьезоэлектрики, воспаление, регенерация, скаффолды, стоматология

**Для корреспонденции:** Анастасия Денисовна Коняева. E-mail: asyakonya95@gmail.com

**Для цитирования:** Коняева А.Д., Варакута Е.Ю., Лейман А.Е., Больбасов Е.Н., Станкевич К.С. Изменения клеточного состава воспалительного инфильтрата и соединительной ткани слизистой оболочки полости рта крыс при регенерации раны с использованием защитного пьезоэлектрического покрытия. Клин. эксп. морфология. 2022;11(1):50–61 (англ.). DOI: 10.31088/CEM2022.11.1.50-61.

**Финансирование.** Исследование выполнено в рамках государственного бюджетного финансирования.

**Конфликт интересов.** Авторы заявляют об отсутствии конфликта интересов.

**Статья поступила** 27.12.2021. **Получена после рецензирования** 25.01.2022. **Принята в печать** 28.02.2022.

## Introduction

Wound healing is a complex process that includes several stages: inflammation, regeneration, and reorganization of the scar [1]. The inflammatory process during wound healing is more pronounced with an open wound, in contrast to the situation when the defect is covered by a protective membrane [2]. This is due to the fact that the wounds of the oral cavity are constantly exposed to aggressive effects from mechanical, physical, chemical, and microbial factors, from which the wound covering protects [3, 4]. At the same time, the presence of piezoelectric properties in membranes favorably affects the prognosis of the regeneration process [5]. We suggested that the cellular composition in the wound defect area at various stages of healing differs depending on the method of injury management. The aim of this research was to study changes in the cellular composition of the oral mucosa during wound regeneration with and without a protective piezoelectric coating.

## Materials and methods

The study was carried out on 50 Wistar rats divided into four groups: the control group of intact rats (n=5) and three experimental groups 1, 2, and 3, each group including 15 rats. The study was approved by the local ethics committee of the Siberian State Medical University (No. 7693/1 from 26.8.2019). The study was carried out in compliance with the principles of humanity set out in the Council Directive (86/609/EEC) and the Declaration of Helsinki. The rats from the experimental groups were subjected to excision of a lip mucous membrane flap with the formation of a wound being 7×4 mm. In the animals of experimental group 1, the defect was open, which corresponded to the traditional method of treating wound surfaces in the oral cavity. In animals of experimental groups 2 and 3, the wound defect was coated with a polymer membrane, fixed along the edges of the wound with simple interrupted sutures (Fig. 1). In the rats of experimental group 3, we used a polymer membrane modified with copper the side with sputtering being on the wound. Surgical intervention was performed under intramuscular sedation with "Zoletil."

The animals were sacrificed on days 3, 7, and 12 of the study by introducing them into hypoxia in a $CO_2$ chamber. We carried out a visual assessment and a photo protocol of the wound with a macroscope. Then, soft tissues were excised from the area of the formed defect to manufacture

*Fig. 1.* Surgical intervention: excision of the lip mucous membrane and subsequent coating of the wound with a polymer membrane

*Рис. 1.* Оперативное вмешательство – иссечение слизистой оболочки губы с закрытием раневого дефекта полимерной мембраной

histological specimens. Material for semi- and ultra-thin sections was taken from the distal part of the wound relative to the central incisors. After that, the material was placed on blocks and marked to define the topography of histological materials.

The materials were placed in a 2.5% glutaraldehyde solution in 0.2 M cacodylate buffer (1:9) for fixation and postfixed in a 1% $OsO_4$ solution for 4 hours in a refrigerator. Dehydration was carried out in ethanol with ascending concentration: the specimens were held in 70% ethanol overnight, then brought to 96% ethanol, and kept twice in acetone for 15 minutes. After dehydration, the specimens were poured into a mixture of epon and araldite M.

Semi- and ultra-thin sections were prepared on an LKB-4 ultratome (LKB Vertriebs GmbH, Sweden). The former were colored with toluidine blue and examined under an optical microscope; the latter sections were contrasted with uranyl acetate and lead citrate and studied using a JEM-1400 electron microscope (JEOL, Japan).

We performed qualitative and quantitative histological assessments and determined the number density (ND) of macrophages (MPs), neutrophils (NPs), fibroblasts (FBs), lymphocytes (LC), plasma cells (PCs), mast cells (MCs), and eosinophils (EPs) per 1 mm$^2$ of section. For each histological specimen, we analyzed 50 fields of view (×900). The indicators were calculated using the Image J program. We verified the normal distribution hypothesis using the Kolmogorov–Smirnov test. Since the distribution of the values of all quantitative traits did not correspond to the normality tests, we used the Kruskal–Wallis one-way analysis of variance with the median test to compare independent samples and the Wilcoxon signed-rank test for paired comparisons. The results were considered statistically significant at $p<0.05$.

**Results**

On day 3, we visualized wound defects in all experimental groups with a macroscope. In experimental group 1, the defects were 21.3±2.3 mm$^2$ large. Visual examination showed asymmetry of the face with buccal region edema on the side of the wound. The surface of the wound was covered with a loose yellowish plaque. After debridement of the wound with a cotton swab moistened with a 0.05% solution of chlorhexidine, we observed bleeding and exposure of the wound surface. The mucous membrane surrounding the wound defect was hyperemic and edematous (Fig. 2A).

In rats of experimental groups 2 and 3, facial asymmetry was not expressed and swelling of the buccal region was not visualized. When we removed the membrane from the wound, we observed defects of 17.8±3.1 mm$^2$ and 16.2±2.2 mm$^2$ in the animals of groups 2 and 3, respectively. In both groups, there was a fibrinous plaque in the center of the wound and a smooth glossy bright pink tissue along the periphery. The plaque was easily removed from the surface of the wound after debridement with a cotton swab moistened with 0.05% chlorhexidine solution; there was no bleeding. Hyperemia and swelling were less pronounced than in group 1 (Fig. 2B).

Histologically, we observed extensive cellular infiltration in the defect areas in all experimental groups on day 3. It was represented by NP (1), MP (2), FB (3), MC (4), PC (5), LC (6), and EP (7). At wound edges, we determined necrotic debris containing fiber fragments and cells (CF) of connective tissue, rod-shaped and spherical bacterial cells (BCs) [Fig. 3A, Fig. 4A, Fig. 4B].

In experimental group 1, ND of NPs reached 2911.5 (2865.0; 2956.0) per 1 mm$^2$ of the section, which was 1.65 and 2.15 times significantly more than in experimental groups 2 and 3 ($p=0.047$), respectively, and 242 times significantly more than in the control group ($p=0.045$) (Table).

In the wound area, mature NPs predominated, which is evidenced by a clearly segmented nucleus (N) with peripherally condensed heterochromatin (HH); nucleoli were absent. Mature NPs were surrounded by fiber and cell fragments (CFs) of connective tissue and bacterial cells (BCs). The NP ultrastructure indicated their high phagocytic activity: multiple granules (Gr), glycogen clumps (Gl), phagolysosomes, and residual bodies (RB) were visualized in the cytoplasm, the cell membrane formed outgrowths (*). At the same time, such organelles as the Golgi complex, rough endoplasmic reticulum, mitochondria (M) were expressed weakly and almost not visualized (Fig. 4B).

In experimental group 1, the ND of MPs was 772.5 (750.2; 788.0) per 1 mm$^2$ of the section, which was 4.7 times higher than in the control group and 1.65 and 2.3 times lower than in experimental groups 2 and 3, respectively ($p=0.039$) (Table).

On ultramicroscopic examination, MP, as well as NP (Fig. 4C) showed signs of high phagocytic activity: multiple outgrowths (*) formed by the cell membrane, a large number of lysosomes (L), phagolysosomes, and residual bodies (RBs) were visualized in the cytoplasm. We ob-

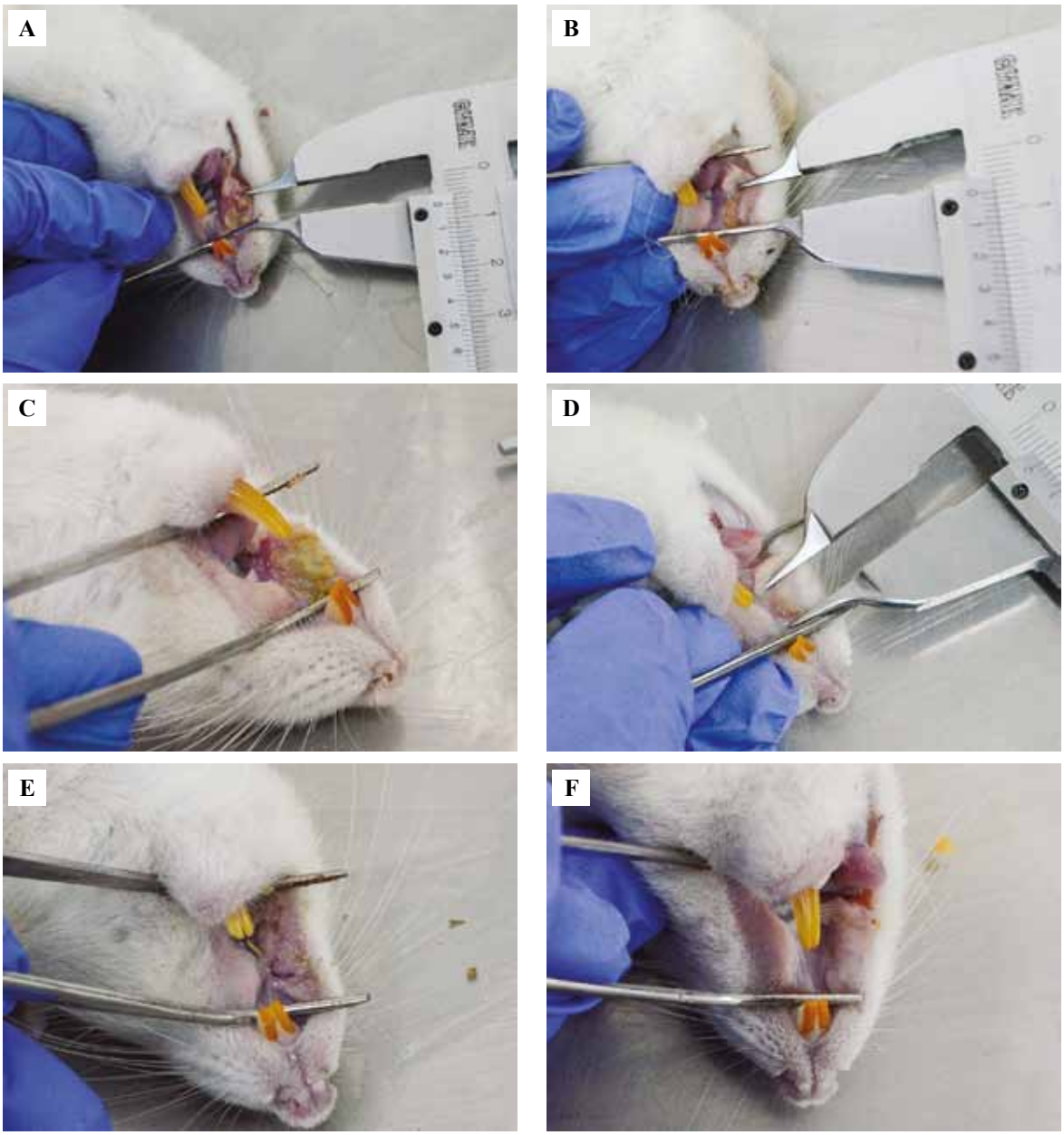


*Fig. 2.* Macrophotographs of the wound defect. A – the wound defect in the buccal area with a hyperemic mucous membrane along the periphery and a fibrinous plaque in the center. Experimental group 1. Day 3. B – the wound defect in the cheek area with a fibrinous plaque in the center. Macroscopic appearance, typical for groups with wound coverage. Experimental group 2. Day 3. C – the wound defect in the buccal area with hyperemic mucous membrane along the periphery and fibrinous plaque in the center. Experimental group 1. Day 7. D – the wound defect in the buccal area with a fibrinous coating in the center. Macroscopic appearance, typical of groups with wound coverage. Experimental group 3. Day 7. E – the scar at the site of a wound defect in the buccal mucosa. Decreased soft tissue volume. Experimental group 1. Day 12. F – the regenerated buccal mucosa at the site of a wound defect. Slight cicatricial deformity, unexpressed decrease in soft tissue volume. Macroscopic appearance, typical of groups with wound coverage. Experimental group 3. Day 12

*Рис. 2.* Макрофотографии раневого дефекта. А – раневой дефект в области щеки крысы с гиперемированной слизистой оболочкой по периферии и фибринозным налетом в центре. 1-я экспериментальная группа. 3-и сутки исследования. В – раневой дефект в области щеки крысы с фибринозным налетом в центре. Макроскопическая картина, характерная для групп с раневым покрытием. 2-я экспериментальная группа. 3-и сутки исследования. С – раневой дефект в области щеки крысы с гиперемированной слизистой оболочкой по периферии и фибринозным налетом в центре. 1-я экспериментальная группа. 7-е сутки исследования. D – раневой дефект в области щеки крысы с фибринозным налетом в центре. Макроскопическая картина, характерная для групп с раневым покрытием. 3-я экспериментальная группа. 7-е сутки исследования. Е – рубец на месте раневого дефекта слизистой оболочки щеки крысы. Снижение объема мягких тканей. 1-я экспериментальная группа. 12-е сутки исследования. F – регенерировавшая слизистая оболочка щеки крысы на месте раневого дефекта. Незначительная рубцовая деформация, невыраженное снижение объема мягких тканей. Макроскопическая картина, характерная для групп с раневым покрытием. 3-я экспериментальная группа. 12-е сутки исследования

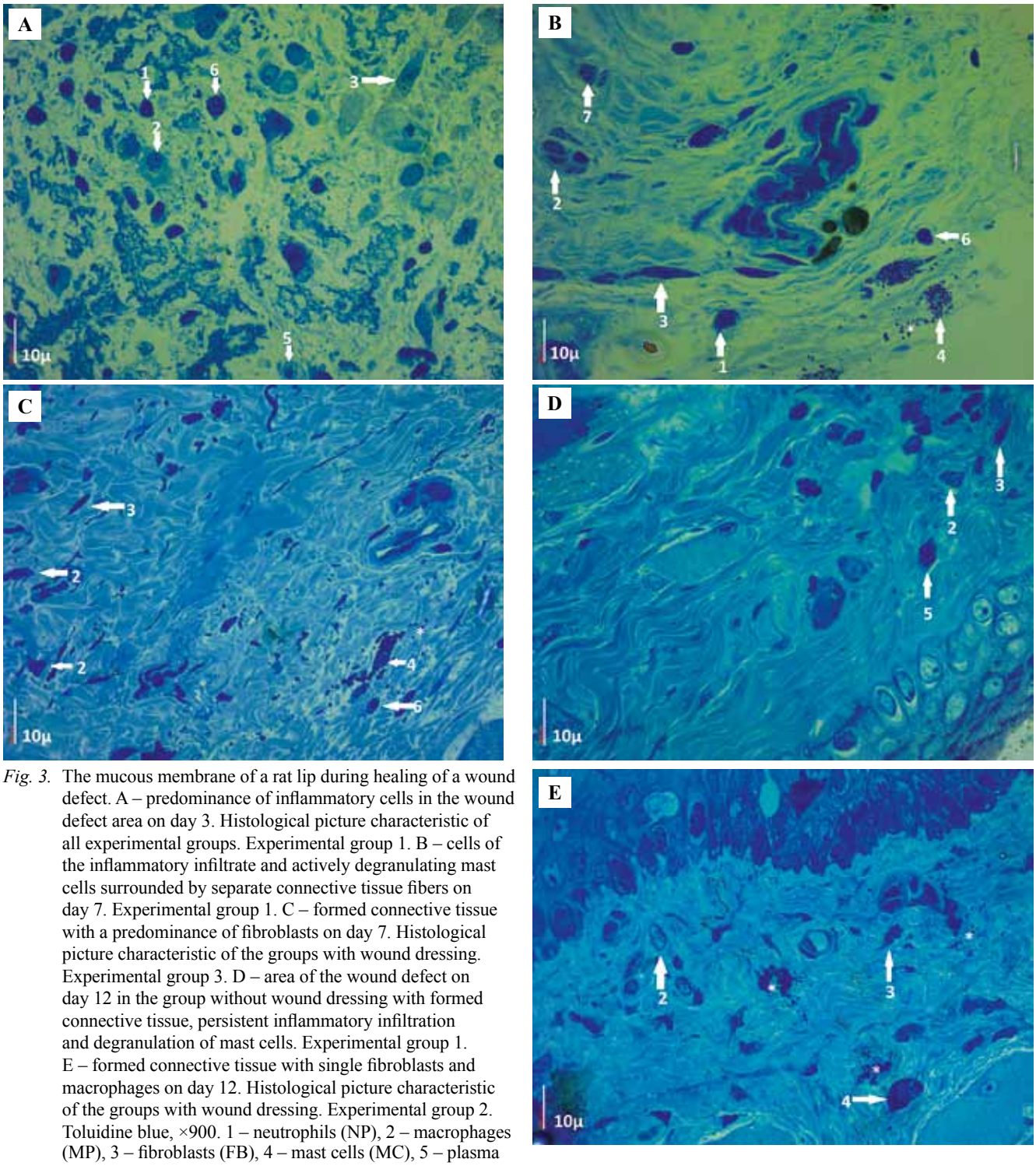


*Fig. 3.* The mucous membrane of a rat lip during healing of a wound defect. A – predominance of inflammatory cells in the wound defect area on day 3. Histological picture characteristic of all experimental groups. Experimental group 1. B – cells of the inflammatory infiltrate and actively degranulating mast cells surrounded by separate connective tissue fibers on day 7. Experimental group 1. C – formed connective tissue with a predominance of fibroblasts on day 7. Histological picture characteristic of the groups with wound dressing. Experimental group 3. D – area of the wound defect on day 12 in the group without wound dressing with formed connective tissue, persistent inflammatory infiltration and degranulation of mast cells. Experimental group 1. E – formed connective tissue with single fibroblasts and macrophages on day 12. Histological picture characteristic of the groups with wound dressing. Experimental group 2. Toluidine blue, ×900. 1 – neutrophils (NP), 2 – macrophages (MP), 3 – fibroblasts (FB), 4 – mast cells (MC), 5 – plasma cells (PC), 6 – lymphocytes (LC), 7 – eosinophils (EP)

*Рис. 3.* Слизистая оболочка губы крысы в ходе заживления раневого дефекта. А – преобладание клеток воспалительного инфильтрата в области раневого дефекта на 3-и сутки исследования. Гистологическая картина, характерная для всех экспериментальных групп. 1-я экспериментальная группа. В – клетки воспалительного инфильтрата и активно дегранулирующие тучные клетки в окружении отдельных соединительнотканных волокон на 7-е сутки исследования. 1-я экспериментальная группа. С – сформированная соединительная ткань с преобладанием клеток фибробластического ряда на 7-е сутки. Гистологическая картина, характерная для 2-й и 3-й экспериментальных групп. 3-я экспериментальная группа. D – область раневого дефекта на 12-е сутки исследования со сформированной соединительной тканью, сохраняющейся воспалительной инфильтрацией и дегрануляцией тучных клеток. 1-я экспериментальная группа. Е – сформированная соединительная ткань с единичными фибробластами и макрофагами на 12-е сутки исследования. Гистологическая картина, характерная для 2-ой и 3-ей экспериментальных групп. 3-я экспериментальная группа. Толуидиновый синий, ×900 1 – НФ, 2 – МФ, 3 – ФБ, 4 – ТК, 5 – ПЦ, 6 – ЛЦ, 7 – ЭФ

*Table | Таблица*

**The number density of cellular components in the wound defect area of the oral mucosa (per 1 mm² of section) | Численная плотность клеточных элементов в области раневого дефекта слизистой оболочки полости рта (в 1 мм² среза)**

| | ND of NP \| ЧП НФ | ND of MP \| ЧП МФ | ND of FB \| ЧП ФБ | ND of MC \| ЧП ТК | ND of PC \| ЧП ПЦ | ND of LC \| ЧП ЛЦ | ND of EP \| ЧП ЭО |
|---|---|---|---|---|---|---|---|
| Control \| Контроль | 12.0 (10.0; 17.7) | 163.0 (158.0; 165.0) | 380.0 (376.0; 391.7) | 45.00 (43.0; 46.0) | 176.0 (173.2; 17.7) | 12.0 (0; 14.0) | 10.0 (0; 20.0) |
| Day 3 \| 3-и сутки | | | | | | | |
| Group 1 \| 1-я группа | 2911.5* (2865.0; 2956.0) | 772.5* (750.2; 788.0) | 3782.0* (3721.0; 3849.5) | 12.0* (12.0; 13.0) | 197.0 (9.0; 10.7) | 161.0* (159.0; 164.0) | 75.0 * (73.0; 77.7) |
| Group 2 \| 2-я группа | 1765.0*# (1745.7; 1793.7) | 1274.0*# (1251.7; 1294.0) | 4464.0* (4418.5; 4505.5) | 17.0* (16.0; 19.0) | 192.0 (89.0; 94.0) | 147.5* (144.0; 149.7) | 55.0* (52.0; 56.0) |
| Group 3 \| 3-я группа | 1355.5*# (1294.0; 1366.5) | 1750.0 *# (1735.2; 1785.5) | 5378.5*# (5346.2; 5465.7) | 17.0* (16.0; 20.0) | 192.0 (88.0; 94.0) | 149.0* (145.0; 152.7) | 47.0* (45.0; 50.0) |
| Day 7 \| 7-е сутки | | | | | | | |
| Group 1 \| 1-я группа | 1148.0* (1128.5; 1171.2) | 1846.0* (1831.2; 1869.0) | 4530.5* (4472.5; 4579.7) | 127.0* (125.0; 131.0) | 73.5* (71.2; 77.7) | 323.0* (319.0; 327.0) | 71.0* (67.2; 72.7) |
| Group 2 \| 2-я группа | 855.5* (791.7; 919.7) | 1470.5* (1435.2; 1488.7) | 5436.0* (5372.7; 5512.2) | 224.5*# (220.2; 321.0) | 98.0*# (95.2; 102.1) | 548.0*# (544.5; 563.0) | 42.0*# (38.0; 44.7) |
| Group 3 \| 3-я группа | 581.0*# (569.7; 585.7) | 1128.0*# (1118.5; 1145.7) | 6136.0*# (6126.0; 6145.0) | 321.0*# (319.0; 327.0) | 127.0# (122.0; 131.0) | 629.0*# (627.2; 635.0) | 29.0*# (25.2; 32.0) |
| Day 12 \| 12-е сутки | | | | | | | |
| Group 1 \| 1-я группа | 457.0* (452.0; 465.0) | 971.0* (947.0; 1138.2) | 2746.5* (2639.0; 2906.0) | 130.0* (125.2; 132.0) | 100.0* (95.0; 102.0) | 226.0* (223.0; 229.0) | 18.0* (16.0; 19.0) |
| Group 2 \| 2-я группа | 99.5*# (95.0; 102.0) | 159.0# (157.2;163.7) | 397.0# (392.2; 400.7) | 45.0# (43.2; 46.0) | 151.0# (145.2; 155.0) | 109.0*# (108.0; 113. 5) | 10# (0; 10.0) |
| Group 3 \| 3-я группа | 12# (12.0; 13.0) | 147,5# (143.0; 149.7) | 397.5# (395.0; 402.0) | 45.0# (43.0; 46.0) | 175.0# (173.0; 177.0) | 935*# (91.0; 95.0) | 10# (10.0; 17.0) |

* – significant differences compared to the control group (p<0.05); # – significant differences compared to group 1 (p<0.05)
ND – numeric density, NP – neutrophils, MP – macrophages, FB – fibroblasts, MC – mast cells, PC – plasma cells, LC – lymphocytes, EP – eosinophils

* – достоверные различия по сравнению с контрольной группой (p<0,05); # – достоверные различия по сравнению с 1-й группой (p<0,05)
ЧП – численная плотность, НФ – нейтрофилы, МФ – макрофаги, ФБ – фибробласты, ТК – тучные клетки, ПЦ – плазмациты, ЛЦ – лимфоциты, ЭФ – эозинофилы

served a large number of mitochondria (M) with clearly structured crypts, as well as an extensive rough endoplasmic reticulum (RER) and the Golgi complex (GC).

In experimental group 1, the ND of granular MCs decreased to 17.0 (16.0; 19.0) per 1 mm² of section, which did not differ from that in experimental groups 2 and 3 (p=0.065) (Table).

ND of EPs did not significantly differ between the experimental groups (p=0.089) and reached 75.0 (73.0; 77.7) per 1 mm² of section for group 1, which was 7.5 times greater than in the control group (p=0.029) (Table).

In all experimental groups, ND of PCs did not significantly differ from that in the control group being 176.0 (173.2; 178.7) per 1 mm² of section (p=0.087) (Table).

In experimental group 1, ND of LCs was 161.0 (159.0; 164.0) per 1 mm² of section and did not differ significantly from that in other experimental groups (p=0.085) but it was 13.4 times higher than in the control group (p=0.036) (Table).

In experimental group 3, ND of FBs reached 5378.5 (5346.2; 5465.7) per 1 mm² of section which was 1.4 times higher than in groups 1 and 2, and 14 times higher than in the control group (p=0.041) (Table).

In all groups, there prevailed young fusiform FBs with moderately developed synthesis organelles: rough endoplasmic reticulum (RER) and the Golgi complex (GC). In the nuclei with small invaginations, HH condensed along the periphery as osmiophilic lumps, and decondensed chromatin was distributed in the central part of the nuclei. Large mitochondria (M) with complexly structured crypts were visualized inside the cytoplasm. Vesicles (V) with suspected procollagen molecules were observed near the cell membrane (PM). On the periphery of the FBs, there were signs of extracellular edema and collagen protofibrils (Fig. 4D).

In animals of group 1, on day 7, there was no facial asymmetry and swelling of the buccal region on the side of the surgical intervention. The wound was 8.2±2.1 mm²,

in the center of which there was a loose fibrinous plaque, which was easily removed after the wound was debrided with a cotton swab moistened with 0.05% chlorhexidine solution. Bleeding from the wound was insignificant. Along the edge of the regenerating surface, we observed a rough matte pink tissue, sharply limited from the normal mucous membrane, which, in turn, was slightly hyperemic and edematous along the edges of the defect. There was a decrease in the soft tissue volume in the wound area which is supposed to follow a consequence of cicatricial deformity of the wound (Fig. 2C).

In groups 2 and 3, there was no facial asymmetry; the wound under the membrane was clean and without plaque. The size of the defect was 4.8±2.1 mm$^2$, which is not significantly different (p=0.065). The mucous membrane around the wound defect was pale pink and nonedematous. Regeneration occurred with sufficient restoration of soft tissue volume (Fig. 2D).

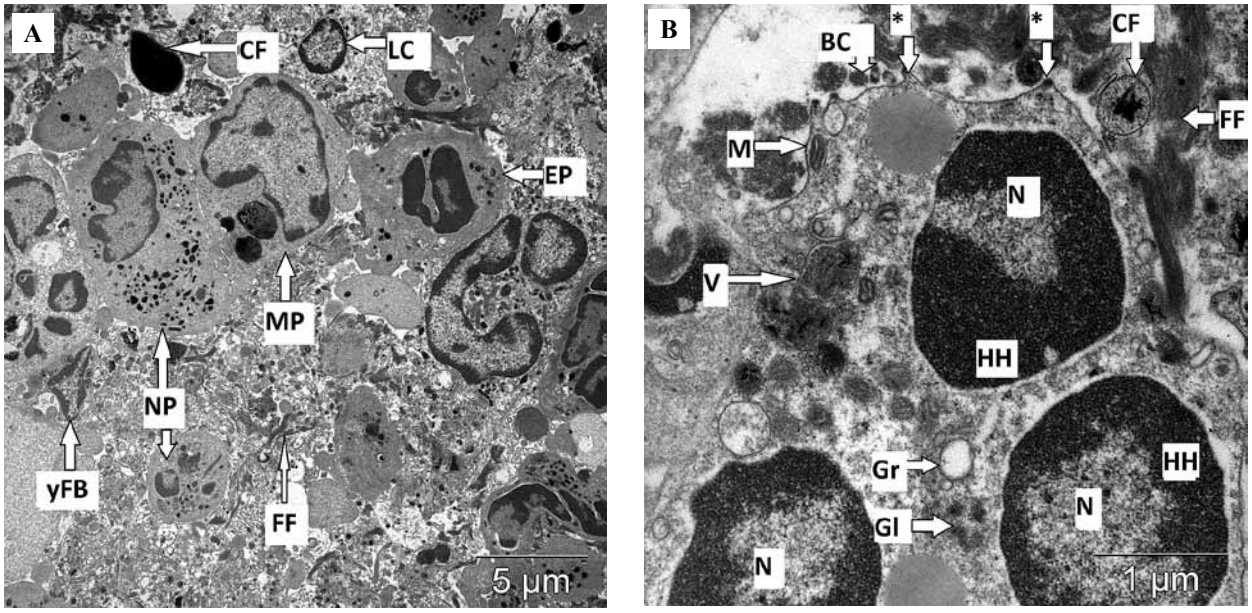


*Fig. 4.* Electron micrographs of cells from the wound defect area.
A – accumulation of inflammatory cells with predominance of polymorphonuclear leukocytes on day 3, ×5000. B – neutrophil from the wound defect area with outgrowths of plasma membrane and phagolysosomes indicating high phagocytic activity on day 3, ×20000. C – macrophage with multiple pronounced synthesis organelles, outgrowths of plasma membrane, phagolysosomes and residual bodies inside the cell on day 3, ×20000. D – young fibroblast with signs of increasing synthetic activity: a large number of mitochondria and pronounced rough endoplasmatic reticulum, cytoplasmic outgrowths on day 3, ×20000. E – degranulating mast cell with low synthetic activity on day 7, ×20000. F – mature fibroblasts with signs of high synthetic activity surrounded by formed collagen networks in groups with wound covering on day 7, ×20000.
G – formed connective tissue with fibrinoid areas at the wound defect site with cells of the fibroblastic and macrophage series on day 12, ×5000.
N – nucleus, HH – heterochromatin, EU – euchromatin, RER – rough endoplasmic reticulum, GC – Golgi complex, M – mitochondria, R – ribosome, PM – plasma membrane, NM – nuclear membrane, L – lysosome, RB – residual bodies, V – vacuole, Vez – vesicle, Gr – granule. Gl – glycogen, FF – fragments of fibers, CF – fragments of cells, FC – fibers of collagen, , FIB – fibrinoid, BC – basal cell of epithelium, * – outgrowths of the cytoplasm

*Рис. 4.* Электронные микрофотографии клеток из области раневого дефекта.
A – скопление клеток воспалительного инфильтрата с преобладанием полиморфноядерных лейкоцитов на 3-и сутки исследования, ×5000. B – нейтрофил из области раневого дефекта на 3-и сутки исследования с выростами плазматической мембраны и фаголизосомами, свидетельствующими о высокой фагоцитарной активности, ×20 000. C – макрофаг с множественными выраженными органеллами синтеза, выростами плазматической мембраны, фаголизосомами и резидуальными тельцами внутри клетки на 3-и сутки исследования, ×20 000. D – юный фибробласт с признаками нарастающей синтетической активности – большим количеством митохондрий и выраженной гЭПР, выростами цитоплазмы на 3-и сутки исследования, ×20 000. E – дегранулирующая тучная клетка с низкой синтетической активностью на 7-е сутки исследования, ×20 000. F – зрелые фибробласты с признаками высокой синтетической активности в окружении сформированных коллагеновых волокон во 2-й и 3-й экспериментальных группах на 7-е сутки исследования, ×20 000. G – сформированная соединительная ткань с участками фибриноида на месте раневого дефекта с клетками фибробластического и макрофагального ряда на 12-е сутки исследования, ×5000
N – ядро, HH – гетерохроматин, EU – эухроматин, RER – гранулярный эндоплазматический ретикулум, GC – комплекс Гольджи, M – митохондрия, R – рибосома, PM – плазматическая мембрана, NM – ядерная мембрана, L – лизосома, RB – резидуальные тельца, V – вакуоль, Vez – везикула, Gr – гранула. Gl – гликоген, FF – обломки волокон, FC – обломки клеток, FC – коллагеновые волокна, Fib– фибриноид, BC – базальная клетка, * – выросты цитоплазмы

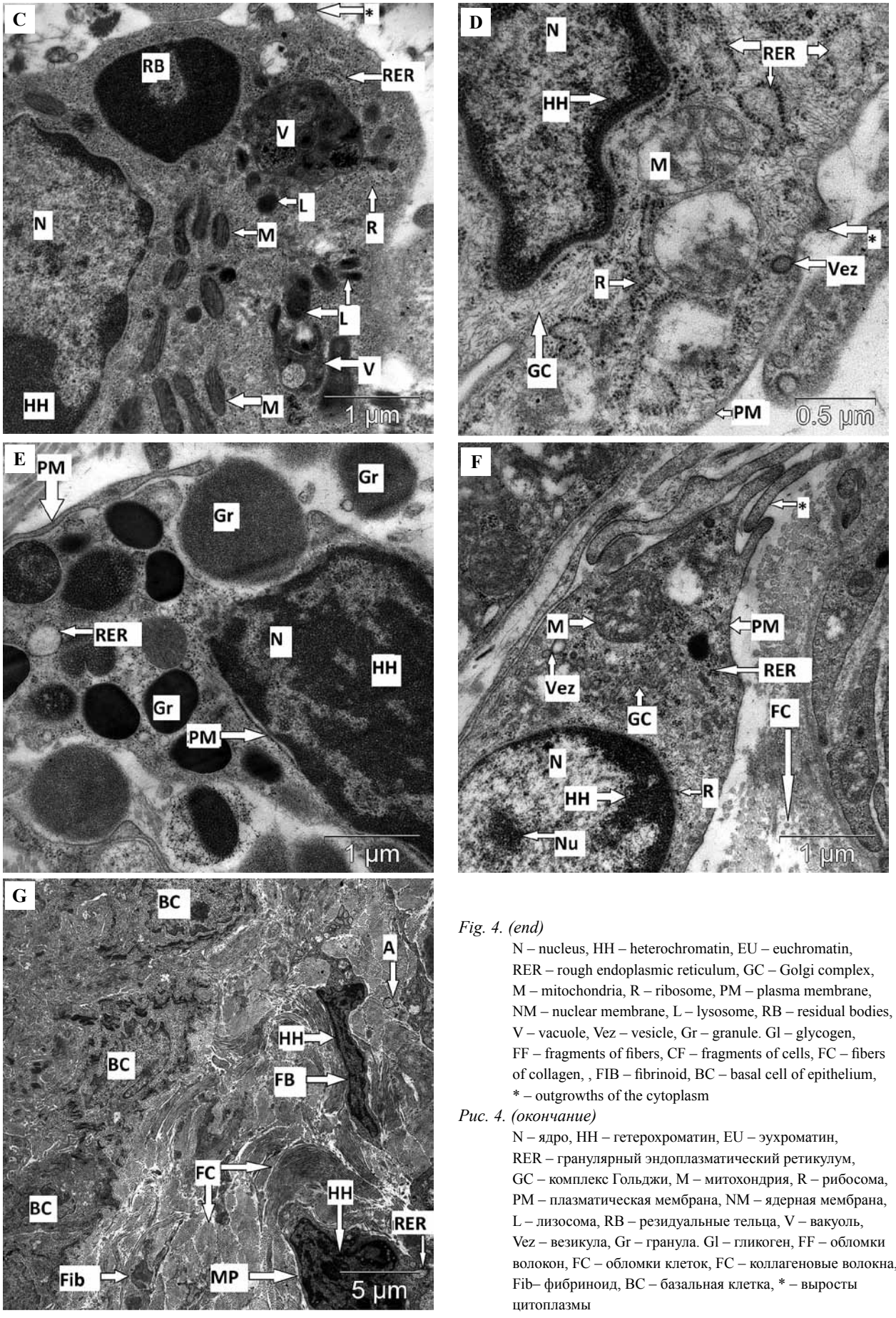


*Fig. 4. (end)*

N – nucleus, HH – heterochromatin, EU – euchromatin, RER – rough endoplasmic reticulum, GC – Golgi complex, M – mitochondria, R – ribosome, PM – plasma membrane, NM – nuclear membrane, L – lysosome, RB – residual bodies, V – vacuole, Vez – vesicle, Gr – granule. Gl – glycogen, FF – fragments of fibers, CF – fragments of cells, FC – fibers of collagen, , FIB – fibrinoid, BC – basal cell of epithelium, * – outgrowths of the cytoplasm

*Рис. 4. (окончание)*

N – ядро, HH – гетерохроматин, EU – эухроматин, RER – гранулярный эндоплазматический ретикулум, GC – комплекс Гольджи, M – митохондрия, R – рибосома, PM – плазматическая мембрана, NM – ядерная мембрана, L – лизосома, RB – резидуальные тельца, V – вакуоль, Vez – везикула, Gr – гранула. Gl – гликоген, FF – обломки волокон, FC – обломки клеток, FC – коллагеновые волокна, Fib– фибриноид, BC – базальная клетка, * – выросты цитоплазмы

On day 7, there preserved cellular composition of the infiltrate (Fig. 3B, C), while the ND of cell populations changed.

We studied ND of NPs in all groups and compared the data to those of day 3. We detected a 2.3-fold decrease in groups 1 and 3 and a 2-fold decrease in group 2 (p=0.042).

In groups 1 and 2, the ND of MPs did not differ significantly and increased 2.4 and 1.3 times, respectively, compared to the figures of day 3 (p=0.033). In group 3 and the control group, this indicator was 1.6 and 11.1 times lower, respectively, than in groups 1 and 2 (p=0.035) (Table).

ND of PCs and LCs changed as well. ND of PCs decreased by 2.7, 1.9, and 1.5 times in experimental groups 1, 2, and 3, respectively (p=0.043). It was 2.4 times lower in group 1 and 1.8 times lower in groups 2 and 3 than in the control group (p=0.034). On the contrary, ND of LCs increased significantly 2, 3.7, and 4.2 times in experimental groups 1, 2, and 3, respectively (p=0.04). It was 27 times higher in group 1 and 52 times greater in groups 2 and 3 than in the control group (p=0.04) (Table).

ND of EPs decreased significantly only in experimental group 3 and was 29.0 (25.2; 32.0) per 1 $mm^2$ of section, which was 1.6 times lower compared to that on day 3, but 2.9 times higher than that in the control group (p=0.029) (Table). In experimental groups 1 and 2, there were no significant differences in comparison with day 3 (p=0.079).

ND of granulated MCs increased 10.6, 13.2, and 18.4 times in groups 1, 2, and 3, respectively, compared to that on day 3 (p=0.022). It was 2.7, 5, and 7.1 times higher in experimental groups 1, 2, and 3, respectively, than in the control group (p=0.033) (Table).

MCs were located mainly near the vessels. Inside the cells, we observed numerous granules of different electron densities, which were partially released into the surrounding tissue by exocytosis. In the cytoplasm, we detected only RER and well visualized mitochondria (M). The nuclei (N) were with a moderate amount of heterochromatin (HC) (Fig. 4E).

ND of FBs was 1.2 times higher compared to that in all experimental groups (p=0.045) on day 3. We observed a 12-fold, 14-fold, and 16-fold increase in FBs in groups 1, 2, and 3, respectively, compared to that in the control group (p=0.047) (Table). At the same time, this indicator in group 3 was 1.35 times higher (p=0.039), whereas the indicator in group 2 did not differ from the group without wound dressing.

In the groups with coating, the branched FBs had a high synthetic activity: euchromatin (Eu) occupied almost the entire area of the nucleus (N). In the cytoplasm, there visualized well-developed RER with dilated cisterns and homogeneous content of average electron density, free polysomes (P) and hypertrophied GC. Micropinocytic vesicles (Vez) migrated from RER and GC, which contained molecules procollagen. The plasma membrane (PM) formed numerous outgrowths (*) for exocytosis. In the surrounding tissues, we found clearly structured collagen fibers (CF) located in different planes (Fig. 4F). In the uncoated group, young fibroblasts still predominated; their ultrastructure remained practically unchanged in comparison with that on day 3.

On day 12, there was no facial asymmetry in all experimental groups. At the site of the wound defect, we observed a scar 4.5±0.3 mm long in group 1 and 1.5±0.2 mm and 1.4±0.2 mm long in groups 2 and 3, respectively. The mucous membrane around the scar was pale pink and nonedematous. In group 1, there was a decrease in the soft tissue volume at the site of the wound defect. In groups 2 and 3, we visualized regeneration with full restoration of soft tissues (Fig. 3E, Fig. 3F).

On day 12, ND of MCs in groups 2 and 3 did not differ significantly from that in the control group and was 2.9 times higher than in group 1 (p=0.025). ND of FBs in the same groups reached control values and was 6.9 times greater than in the uncoated group (p=0.021) (Table). In groups 2 and 3, the cells were elongated and narrow. Heterochromatin (HH) was detected in the nuclei, indicating a decrease in the functional activity of cells. The organelles were well defined; the cisterns of the GC and RER were not dilated. We did not detect extracellular edema around the cells, but observed clearly organized collagen fibers, among which there were complexes of myelin-free nerve fibers united by Schwann cells (A) (Fig. 4F).

On day 12, neutrophilic infiltration was still preserved in experimental group 1 (Fig. 3E). Their ND was 4.6 times higher than in group 2 and 38 times higher than in group 3 and the control group (p=0.012). In groups 2 and 3, this indicator reached the control values (Table).

In groups 2 and 3, ND of MPs reached the control group values of 159.0 (157.2; 163.7) and 147.5 (143.0; 49.7), respectively, which was 6 times lower than in group 1 (p=0.022) (Table).

In the uncoated group, we detected macrophages (MPs) with signs of dysfunction: the nuclei contained fragmented heterochromatin (HH); organelles inside the cells were not expressed; GC and RER lay as separate cisterns; and there was a large number of phagolysosomes and residual bodies in the cytoplasm. MPs were located near clusters of fibrinoid (Fib) and surrounded by osmiphilic granules (presumably by mast cells and neutrophils) and in the lamina propria near the basal layer (BC) of the epithelium (Fig. 3G). The fibrinoid formed a coach for the migration of epithelial cells during re-epithelialization of the wound, which would subsequently undergo phagocytosis by macrophages. At the same time, their phagocytic activity decreased: invaginations and outgrowths of the cytoplasm decreased in size and there were practically no digestive vacuoles inside the cells.

ND of PCs in the coated groups did not significantly differ from that in the control group but was 1.75 times higher than in group 1 (p=0.038). Compared to the data obtained on day 7, ND of LCs decreased by 1.42 times in group 1, 5 times in group 2, and 6.7 times in group 3, respectively (p=0.045). However ND of LCs did not reach the control values (Table).

In groups 2 and 3, ND of EPs reached the control values and was 1.8 times greater than in group 1 (p=0.038) (Table).

Thus, on day 12, almost all the studied parameters reached the control values in groups with wound dressing, except for ND of NPs and LCs for group 2 and ND of LCs for group 3. In the group with no wound dressing, no indicators reached the control values.

**Discussion**

During the regeneration of the oral mucosa wound defect, there occured a complex of intercellular interactions, the mechanism of which is still to be fully understood. These interactions aim at restoring the integrity of the tissue and protecting it from aggressive influence [6]. The defect restoration was carried out as a result of the coordinated activity of FBs, MPs, MCs, agranulocytes, and granulocytes [7].

The 1st stage of wound healing proceeded with a predominance of the inflammatory reaction for the first three days. It was aimed at limiting the defect containing necrotic tissues, microorganisms and elements of primary contamination from healthy tissues by removal of these pathological products and elimination of the consequences of damage [8].

Primarily, the main role in inflammation belonged to NPs, the ND of which increased significantly in all experimental groups. They alomost did not occur in the intact mucous membrane. NPs cleaned the wound defect from tissue dendrite and microorganisms and secreted biologically active substances necessary for the migration of other cellular elements into the wound [6]. Electron microscopy showed an increase in their phagocytic activity.

According to modern concepts of the inflammatory process, neutrophilic infiltration was replaced by macrophage for the implementation of phagocytosis [6]. Releasing biologically active substances, MPs influenced the proliferation of FBs. In addition, they synthesized the extracellular matrix independently [9, 10].

When using a polymer membrane, especially in the group with copper spraying membrane, we observed a more active change from neutrophilic to macrophage infiltration, which can indicate a more rapid abatement of the inflammation phase. In addition to the active phagocytic processes, MPs had the ultrastructure signs indicating a high level of synthetic processes associated with the formation of biologically active substances determining inflammatory and regenerative processes [11].

A decrease in ND of MCs occurred as a result of their degranulation, during which biologically active substances were released to regulate the vascular wall tone and the migration of other cells to the inflammation focus [12, 13]. MPs were predominantly located near the lumen of the vessels with interstitial edema.

In all experimental groups, an increase in the NDs of PCs, LCs, and EPs was due to tissue metabolism and acid-base balance was disturbed as a result of edema, which led to the activation of these cell populations in the wound. They participated in the destruction of microorganisms and due to the release of biologically active substances attracted cells of the inflammatory infiltrate into the wound. The role of EPs is not fully understood, but they are supposed to play a role in the anti-infectious protection of the wound [14–16].

Simultaneously with the inflammation phase, there occurred the formation of granulation tissue at the wound defect site. In this process, FBs produced the components of the intercellular substance. In this regard, their ND increased.

On day 7, the cellular composition of the infiltrate was preserved.

The leading role in the inflammatory process was passed to MPs, which became the dominant population in comparison with NPs. This was due to the fact that, in addition to the immune function, including phagocytosis of dead NPs [17], MPs influenced the proliferation of FBs, playing an important role in the development of connective tissue [18, 19].

At this stage, an increase in the ND of MCs was a result of their migration to the wound defect zone. Active migration of MCs into the wound was probably facilitated by the piezoelectric properties of the protective membrane; therefore, the cells of this population were more abundantly present in experimental groups 2 and 3 compared to those in the group group without coating. The appearance of MCs at the wound defect site in this phase was most likely due to the fact that they played a significant role in the formation of loose connective tissue [20].

On day 7, proliferation became the dominant process. In the groups where polymer membranes were used to protect the wound defect, the number of FBs increased in comparison with that in the group group with the conventional treatment, where the formation of loose fibrous connective tissue was violated by constant trauma because of chemical and mechanical irritators.

The next stage of wound regeneration occurring on day 12 was scar reorganization, where the interaction between MCs and FBs was of primary importance. With an increased content of the former, a pronounced formation of fibrous tissue and keloid scars were observed, which we detected in the group without wound defect protection [21]. The persistence of macrophage infiltration and their ultrastructural abnormalities in the uncoated group were a poor prognostic sign because they were prerequisites for the development of cicatricle changes [22]. LCs took part in the restructuring of the scar as well, releasing biologically active substances that affected the termination of the proliferation of FBs, that is why their ND increased in all experimental groups [23].

In all experimental groups, the wound healing process was based on a complex interaction of cell populations at the defect site, which determined the speed and quality of wound healing. Knowledge of these mechanisms and the ability to modulate them can optimize the process of wound management [4, 24, 25]. The present research

demonstrated that the use of polymer membranes, especially with copper deposition, contributed to a more physiological change from one cell population to another and their cascade interaction during wond healing.

## Conclusion

We identified the patterns of changes in the cellular composition of a wound defect during regeneration. The use of wound dressing contributed to reduced regeneration time, which was observed during the analysis of changes in cell populations at different stages of healing. For example, in groups with wound dressing, the replacement of neutrophilic with macrophage infiltration was more intensive, and this indicated a decrease in the inflammation. When the wound defect was closed, the proliferation was more active, which can be argued based on changes in the number density of fibroblasts and their ultrastructural structure. Moreover, in the groups with wound dressing, on day 12, the numeral density of macrophages reached control values in contrast to the group without it. It was a marker of scar tissue formation in experimental group 1. Lymphocytes and plasma cells were active in groups with coating; they also participated in the reorganization of the scar at the final stages of wound healing.

Thus, the closure of the oral mucosa wounds with polymer piezoelectric membranes had a positive effect on the restoration of the qualitative and quantitative cellular composition of the tissue, and, supposedly, reduced the risk of postoperative complications.

## Compliance with ethical principles

The study was approved by the local ethics committee of the Siberian State Medical University (No. 7693/1 from 26.8.2019). The study was carried out in compliance with the principles of humanity set out in the Council Directive (86/609/EEC) and the Declaration of Helsinki.

**Author contributions**

Conceived the study and designed the experiment – A.D. Koniaeva, E.Yu. Varakuta, E.N. Bolbasov, K.S. Stankevich.
Collected the data and performed the analysis – A.D. Koniaeva, A.E. Leiman.
Wrote the paper – A.D. Koniaeva, E.Yu. Varakuta.
Edited the manuscript – A.D. Koniaeva, E.Yu. Varakuta, E.N. Bolbasov, K.S. Stankevich.

**Вклад авторов**

Концепция и дизайн исследования – А.Д. Коняева, Е.Ю. Варакута, Е.Н. Больбасов, К.С. Станкевич.
Сбор и обработка материала – А.Д. Коняева, А.Е. Лейман.
Написание текста – А.Д. Коняева, Е.Ю. Варакута.
Редактирование – А.Д. Коняева, Е.Ю. Варакута, Е.Н. Больбасов, К.С. Станкевич.

## References/Литература

1. *Rodrigues M, Kosaric N, Bonham CA, Gurtner GC.* Wound healing: A cellular perspective. Physiol Rev. 2019;99(1):665–706. DOI: 10.1152/physrev.00067.2017.
2. *Badaraev AD, Koniaeva AD, Krikova SA, Shesterikov EV, Bolbasov EN, Nemoykina AL, Tverdokhlebov SI.* Piezoelectric polymer membranes with thin antibacterial coating for the regeneration of oral mucosa. Applied Surface Science. 2020;504:144068. DOI: 10.1016/j.apsusc.2019.144068.
3. *da Silveria Teixeira D, de Figueiredo MAZ, Cherubina K, de Oliveira SD, Salum FG.* The topical effect of chlorhexidine and povidone-iodine in the repair of oral wounds. A review. Stomatologija. 2019;21(2)35–41. PMID:32108654.
4. *Konyaeva AD, Varakuta EY, Leiman AE, Badaraev AD, Bol'basov EN.* Effectiveness of non-woven piezoelectric polymer membrane application based on a co-polymer of vinylidene fluoride with tetrafluoroethylene for oral wound closure. Journal of Anatomy and Histopathology. 2020;9(2):40–45 (In Russ.). DOI: 10.18499/2225-7357-2020-9-2-40-45.
*Коняева А.Д., Варакута Е.Ю., Лейман А.Е., Бадараев А.Д., Больбасов Е.Н.* Эффективность использования нетканых пьезоэлектрических полимерных мембран на основе сополимера винилиденфторида с тетрафторэтиленом для закрытия раневых дефектов слизистой оболочки полости рта. Журнал анатомии и гистопатологии. 2020;9(2):40–45. DOI: 10.18499/2225-7357-2020-9-2-40-45.
5. *Wang PH, Huang BS, Horng HC, Yeh CC, Chen YJ.* Wound healing. J Chin Med Assoc. 2018;81(2):94–101. DOI: 10.1016/j.jcma.2017.11.002.
6. *Periera D, Sequera I.* A scarless healing tale: Comparing homeostasis and wound healing of oral mucosa with skin and oesophagus. Front Cell Dev Biol. 2021;(9):682143. DOI:10.2289/fcell.2021682143.
7. *Xiao T, Yan Z, Xiao S, Xia Y.* Proinflammatory cytokines regulate epidermal stem cells in wound epithelialization. Stem Cell Res Ther. 2020;11(1):232. DOI: 10.1186/s13287-020-01755-y.
8. *Avishai E, Yeghiazaryan K. Golubnitschaja O.* Impaired wound healing: Facts and hypotheses for multi-professional considerations in predictive, preventive and personalised medicine. EPMA J. 2017;8(1):23–33. DOI: 10.1007/s13167-017-0081-y.
9. *Serra MB, Barroso WA, da Silva NN, Silva SDN, Borges ACR, Abreu IC et al.* From inflammation to current and alternative therapies involved in wound healing. Int J Inflam. 2017;2017:3406215. DOI: 10.1155/2017/3406215.
10. *Kotwal GJ, Chien S.* Macrophage differentiation in normal and accelerated wound healing. Results Probl Cell Differ. 2017;62:353–64. DOI: 10.1007/978-3-319-54090-0_14.
11. *Shapouri-Moghaddam A, Mohammadian S, Vazini H, Taghadosi M, Esmaeili SA, Mardani F et al.* Macrophage plasticity, polarization, and function in health and disease. J Cell Physiol. 2018;233(9):6425–40. DOI: 10.1002/jcp.26429.
12. *Komi DEA, Rambasek T, Wöhrl S.* Mastocytosis: From a molecular point of view. Clinic Rev Allerg Immunol. 2018;54(3):397–411. DOI:10.1007/s12016-017-8619-2.
13. *Komi DEA, Khomtchouk K, Santa Maria PL.* A review of the contribution of mast cells in wound healing: Involved molecular and cellular mechanisms. Clin Rev Allergy Immunol. 2020;58(3):298–312. DOI: 10.1007/s12016-019-08729-w.
14. *Coden ME, Berdnikovs S.* Eosinophils in wound healing and epithelial remodeling: Is coagulation a missing link? J Leukoc Biol. 2020;108(1):93–103. DOI: 10.1002/JLB.3MR0120-390R.
15. *Wang X, Balaji S, Steen EH, Li H, Rae MM, Blum AJ et al.* T lymphocytes attenuate dermal scarring by regulating inflammation,

neovascularization, and extracellular matrix remodeling. Adv Wound Care (New Rochelle). 2019;8(11):527–37. DOI: 10.1089/wound.2019.0981.
16. *Sîrbulescu RF, Boehm CK, Soon E, Wilks MQ, Ilieş I, Yuan H et al.* Mature B cells accelerate wound healing after acute and chronic diabetic skin lesions. Wound Repair Regen. 2017;25(5):774–91. DOI: 10.1111/wrr.12584.
17. *Rousselle P, Braye F, Dayan G.* Re-epithelialization of adult skin wounds: Cellular mechanisms and therapeutic strategies. Adv Drug Deliv Rev. 2019;146:344–65. DOI: 10.1016/j.addr.2018.06.019.
18. *Kloc M, Ghobrial RM, Wosik J, Lewicka A, Lewicki S, Kubiak JZ.* Macrophage functions in wound healing. J Tissue Eng Regen Med. 2019;13(1):99–109. DOI: 10.1002/term.2772.
19. *Smigiel KS, Parks WC.* Macrophages, wound healing, and fibrosis: Recent insights. Curr Rheumatol Rep. 2018;20(4):17. DOI: 10.1007/s11926-018-0725-5.
20. *Alim MA, Peterson M, Pejler G.* Do mast cells have a role in tendon healing and inflammation? Cells. 2020;9(5):1134. DOI: 10.3390/cells9051134.
21. *Ud-Din S, Wilgus TA, Bayat A.* Mast cells in skin scarring: A review of animal and human research. Front Immunol. 2020;11:552205. DOI: 10.3389/fimmu.2020.552205.
22. *Xu X, Gu S, Huang X, Ren J, Gu Y, Wei C et al.* The role of macrophages in the formation of hypertrophic scars and keloids. Burns Trauma. 2020;8:tkaa006. DOI: 10.1093/burnst/tkaa006.
23. *Carlavan I, Bertino B, Rivier M, Martel P, Bourdes V, Motte M et al.* Atrophic scar formation in patients with acne involves long-acting immune responses with plasma cells and alteration of sebaceous glands. Br J Dermatol. 2018;179(4):906–17. DOI: 10.1111/bjd.16680.
24. *Li P, Ruan L, Wang R, Liu T, Song G, Gao X et al*. Electrospun scaffold of collagen and polycaprolactone containing ZnO quantum dots for skin wound regeneration. J Bionic Eng. 2021;18(6):1378–90. DOI: 10.1007/s42235-021-00115-7.
25. *Rodrigues M, Kosaric N, Bonham CA, Gurtner GC.* Wound healing: A cellular perspective. Physiol Rev. 2019;99(1):665–706. DOI: 10.1152/physrev.00067.2017.

**Authtor information**

Anastasiia D. Koniaeva – Teaching Assistant, Human Anatomy Department with a course of Topographic Anatomy and Operative Surgery, Siberian State Medical University.
https://orcid.org/0000-0002-9708-1948

Elena Yu. Varakuta – Dr. Sci. (Med.), Head of the Human Anatomy Department with a course of Topographic Anatomy and Operative Surgery, Siberian State Medical University.
https://orcid.org/0000-0003-3173-5336

Arina E. Leiman – 4th-year student, General Medicine Department, Siberian State Medical University.
https://orcid.org/0000-0002-9959-1546

Eugeniy N. Bolbasov – Cand. Sci. (Engineering), Senior Researcher, Laboratory of Hybrid of Biomaterials, National Research Tomsk Polytechnic University.
https://orcid.org/0000-0002-6113-1835

Ksenia S. Stankevich – Master's Degree Student, Chemistry and Biochemistry Department, Montana State University.
https://orcid.org/0000-0002-6701-7582

**Информация об авторах**

Анастасия Денисовна Коняева – ассистент кафедры анатомии человека с курсом топографической анатомии и оперативной хирургии Сибирского государственного медицинского университета.

Елена Юрьевна Варакута – доктор медицинских наук, заведующая кафедрой анатомии человека с курсом топографической анатомии и оперативной хирургии Сибирского государственного медицинского университета.

Арина Евгеньевна Лейман – студентка 4-го курса лечебного факультета Сибирского государственного медицинского университета.

Евгений Николаевич Больбасов – кандидат технических наук, старший научный сотрудник лаборатории гибридных биоматериалов Национального исследовательского Томского политехнического университета.

Ксения Сергеевна Станкевич – магистрант факультета химии и биохимии, Государственный университет штата Монтана, США.